China Ocean Eng., 2023, Vol. 37, No. 1, P. 73–84
DOI: https://doi.org/10.1007/s13344-023-0007-5, ISSN 0890-5487
http://www.chinaoceanengin.cn/ E-mail: coe@nhri.cn

Hydrodynamic Characteristics of Three-Bucket Jacket Foundation for Offshore Wind Turbines During the Lowering Process

ZHANG Pu-yang[a, b, *], QI Xin[a, b], WEI Yu-mo[a, b], ZHANG Sheng-wei[a, b], LE Cong-huan[a, b], DING Hong-yan[a, b]

[a] State Key Laboratory of Hydraulic Engineering Simulation and Safety, Tianjin University, Tianjin 300072, China

[b] School of Civil Engineering, Tianjin University, Tianjin 300072, China

Received July 1, 2021; revised December 21, 2022; accepted January 3, 2023

Abstract

The three-bucket jacket foundation is a new type of foundation for offshore wind turbine that has the advantages of fast construction speed and suitability for deep water. The study of the hoisting and launching process is of great significance to ensure construction safety in actual projects. In this paper, a new launching technology is proposed that is based on the foundation of the three-bucket jacket for offshore wind turbine. A complete time domain simulation of the launching process of three-bucket jacket foundation is carried out by a theoretical analysis combined with hydrodynamic software Moses. At the same time, the effects of different initial air storage and sea conditions on the motion response of the structure and the hoisting cable tension are studied. The results show that the motion response of the structure is the highest when it is lowered to 1.5 times the bucket height. The natural period of each degree of freedom of the structure increases with the increase of the lowering depth. The structural motion response and the hoisting cable tension vary greatly in the early phases of Stages I and III, smaller in Stage II, and gradually stabilize in the middle and late phases of Stage III.

Key words: three-bucket jacket foundation, time domain simulation, hoisting construction, motion response, offshore wind turbine

Citation: Zhang, P.Y., Qi, X., Wei, Y.M., Zhang, S.W., Le, C.H., Ding, H.Y., 2023. Hydrodynamic characteristics of three-bucket jacket foundation for offshore wind turbines during the lowering process. China Ocean Eng., 37(1): 73–84, doi: https://doi.org/10.1007/s13344-023-0007-5

1 Introduction

The declining reserves of traditional energy sources such as petroleum and coal, and the increasingly severe ecological and environmental problems in the international society call for a reduction in the use of fossil fuels, which can decrease the resulting greenhouse gas emissions. Vigorous development of renewable energy has become the priorities of several countries around the world. Renewable energy, such as hydro energy, wind energy, solar energy, and tidal energy, is a resource that can be used sustainably.

Compared with renewable energy sources such as nuclear energy, solar energy, tidal energy and biomass energy, wind energy technology is relatively mature, and its cost is gradually declining. It is one of the most promising forms of clean energy and it is expected that the development and utilization of this energy both at onshore and offshore locations will significantly slow down global warming and reduce CO_2 emissions (Zou et al., 2023). Compared with the onshore energy, the offshore wind energy is close to the power load center, does not occupy land resources, and has the advantages of high wind speed, high output, stable wind power, low turbulence intensity and low noise. The exploitations of ocean resources have been stimulated to meet the increasing needs for energy (Zhang et al., 2022). The development of offshore wind power has become the main priority of many countries to promote energy transition policies, and an important way to deal with climate change.

Bottom-fixed foundations, such as monopile, jacket, suction bucket and gravity-based foundation, are used for developing offshore wind energy units in shallow water (Shi et al., 2023). The multi-bucket jacket foundation with the combination of suction bucket and jacket is considered to be the most promising form of offshore wind turbine foundation in the future. There are many excellent wind resource sites in the waters of China with water depths of more than 30 m. In these areas, jacket foundation is the most efficient and economical wind turbine foundation. In general, the weight of the multi-bucket jacket foundation is low, and the launching and installation can be completed by a crane vessel. However, a comprehensive study should be conducted before

Foundation item: The work was financially supported by the National Natural Science Foundation of China (Grant No. 52171274).
*Corresponding author. E-mail: zpy_td@163.com

formally carrying out the launching and installation operations in order to ensure the safety of personnel and lifting equipment. The multi-bucket jacket foundation has a suction bucket at the lower part, which is unique compared with other foundations. Part of the air can be retained and compressed in the suction bucket during the lowering process, and the liquid level difference between the inside and outside of the bucket forms an air cushion with a certain air pressure to provide the suction bucket with upward buoyancy. The floating structure provides buoyancy through the air pressure generated by the internal air cushion. Compared with the ordinary solid floating body, the multi-bucket jacket foundation is equivalent to adding an air cushion spring on the water cushion spring. In the floating structures, the earliest use of air cushion was in hovercraft design. It is based on the principle of using high-pressure air to form an air cushion between the bottom of the ship and the water surface (or ground), so that all or part of the hull is uplifted to achieve high-speed navigation.

Seidl (1980) first conducted model tests on a variety of air floating structures, including single-cabin air floating structures and small multi-cabin air cushion structures. The author introduced airbag coefficients to describe the air-water ratio inside the structural air tank. Pinkster (1997) and van Kessel and Ikoma et al. (2012) compared and analyzed the difference between large air floating structures and solid floating structures of the same size in terms of the wave moment and structural load. The authors discovered that the existence of air cushions could reduce the wave excitation force and moment, especially under the low-frequency incident wave condition. Pinkster et al. (1998) used the linear potential flow theory to test and simulate the three-dimensional model of the air floating structure.

Cheung et al. (2000) designed a multi-bucket air floating structure, in which the bottom of each bucket could be opened or sealed to provide buoyancy. The thickness of the bucket wall was considerably smaller than the diameter. The structure can be applied to wave power generation devices, breakwaters, floating airports or military bases, and was verified by experiments and theoretical calculations. Ikoma et al. (2002) proved that the floating structure with air cushion could reduce the hydro-elastic response, and used an integral equation to analyze the movement of the air floating structure under regular waves. Thiagarajan and Morris-Thomas (2006) used the simplified linear wave theory to obtain the heave and pitch responses of the air cushion structure under the action of regular waves. Koo (2009) used numerical wave flume to study the influence of air cushion damping effect of air floating breakwater on structural motion and wave propagation mode.

He et al. (2012) designed a box-type floating breakwater with an air cushion that has an opening at the bottom of the periphery. The research results showed that the water body part of the air cushion structure on both sides could effectively slow down the structural response under regular waves and increase the moment of inertia of the structure. Furthermore, it could effectively reduce the radiation wave generated by the movement of the back wave area of the breakwater. Henriques et al. (2013) and He et al. (2013) further studied the application of this structure in wave power generation devices and expanded the application function of floating breakwater. Ikoma et al. (2013) studied the influence of different subdivision forms and sizes on the dynamic response of the structure. The authors suggested that the single-cabin air floating structure should be subdivided to increase the hydrostatic dynamic stability and reduce sloshing. van Kessel (2010) studied large air floating structures and proposed the idea that the heave motion state could be changed by changing the air pressure in the bucket. This idea was verified experimentally.

Gordon et al. (2013) used simulation of marine operation (SIMO) to conduct time domain simulation of the lowering of suction piles through the splashing zone. The model coupled the structure of the crane vessel, cable, hook and suction pile. The sensitivity of the cable tension to the lowering speed, hydrodynamic coefficient and size of the suction pile was analyzed and compared with other results. Bertelsen (2014) studied the dynamic air cushion pressure when the suction anchor was lowered in the splash zone. The author established a theoretical model of the dynamic air cushion pressure by using the nonlinear continuity equation of the air cushion. Tassin et al. (2013) studied the process of entering and leaving water by the objects with time-varying shapes through numerical modeling.

The above studies mainly focus on the motion mechanism of the air floating body structure under the influence of the air cushion effect and the coupled motion of multiple rigid bodies in the wave environment. The foundation of the multi-bucket jacket has generally a low weight, strong structure, and is stable. It can be installed in an integrated manner by the crane vessel. However, during the lowering process, the foundation may be affected by wind pressure, waves and current impact pressure, resulting in movement on the six degrees of freedom that poses a threat to the hoisting stability. Due to the real-time changes of the hydrodynamic characteristics of the structure (natural period, RAO, etc.), the structure will have different motion responses at different positions. Therefore, it is highly necessary to carry out hydrodynamic analysis for each position.

In this paper, the hydrodynamic software Moses is used in the time domain to study the variation law of the motion response and the hoisting cable tension of the lowering process of the three-bucket jacket foundation. The effects of the wave incident direction, spectral peak period and different initial gas storage inside the suction bucket were considered. And the influence of the air cushion structure on the dynamic lowering process of the multi-bucket jacket foundation is studied.

2 Theory of air cushion and model design

During the lowering process, part of the air can be retained and compressed in the suction bucket. The liquid level difference between the inside and outside of the bucket forms an air cushion with a certain air pressure that provides the suction bucket with upward buoyancy. For the convenience of analysis, the lowering process is divided into three stages as follows.

Stage I: The air valve is opened, and the pressure inside the bucket is considered to be the same as the atmospheric pressure outside the bucket. Only the steel plate on the bucket wall provides a small amount of buoyancy.

Stage II: The air valve is closed and the initial state is reached. Subsequently, the air cushion forms and gradually increases during the lowering process. The air pressure in the bucket begins to rise, and the buoyancy of the air cushion on the structure gradually increases.

Stage III: The water surface does not exceed the head cover of the bucket and the air pressure in the bucket continues to rise. However, the thickness of the air cushion in the bucket and the buoyancy of the air cushion on the structure gradually decrease.

Fig. 1 shows the lowering process. The initial air storage refers to the ratio of air in the bucket to the total volume of the bucket when the foundation of the three-bucket jacket is in the initial position (Position B). When the top of the bucket is above the water surface, the height h_w of the air cushion during the lowering process increases with the lowering operation of the structure. When the top of the bucket reaches the water surface (Position D), h_w becomes the maximum, which means the air buoyancy reaches its maximum value. When the bucket completely enters the water (Position E), h_w decreases as the structure descends, and the air buoyancy decreases gradually.

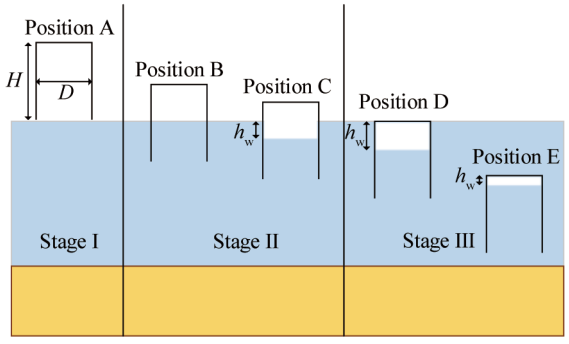

Fig. 1. Lowering process of the suction bucket.

During the lowering process, it can be considered that the temperature and total amount of air in the bucket do not change due to the slow lowering speed. Therefore, the air in the bucket at any position satisfies the following expressions:

$$P_0V_0 = P_1V_1; \tag{1}$$

$$V_0 = \frac{1}{4}\pi D^2 H\beta. \tag{2}$$

In the above equations, P_0 is the standard atmospheric pressure that is equal to 1.01×10^5 Pa, V_0 is the initial air storage, and P_1 and V_1 are the pressure and air volume, respectively during the descending process. Furthermore, D and H represent the diameter and height of the bucket, respectively, and β is the percentage of air storage in the volume of the bucket.

The pressure and volume of the air at any position satisfy the following expression:

$$P_1 = \begin{cases} \gamma_w h_w, & d < H \\ \gamma_w (d - H + h_w), & d \geqslant H \end{cases} \tag{3}$$

$$V_1 = \begin{cases} \frac{1}{4}\pi D^2 (H - d + h_w), & d < H \\ \frac{1}{4}\pi D^2 h_w, & d \geqslant H \end{cases} \tag{4}$$

In the above equations, γ_w is the unit density of seawater, which is equal to 1.0045×10^4 N/m^3, h_w is the height of the air cushion, and d is the distance between the bottom of the bucket and the water surface.

The buoyancy of the structure is directly related to h_w. Ignoring the buoyancy of bucket wall and the rod, the hoisting cable tension in still water can be obtained by the following equations:

$$T = G - F_{buo}; \tag{5}$$

$$F_{buo} = \frac{3}{4}\pi D^2 h_w \gamma_w. \tag{6}$$

In the above expressions, T is the total tension of the hoisting cable, G is the total gravity of the structure and F_{buo} is the air buoyancy.

Incorporating Eqs. (2), (3), (4) and (6) into Eq. (5), the relationship between T and d under different initial air storage values can be obtained without including the buoyancy of the jacket and the buoyancy generated by the bucket wall.

Fig. 2 shows the calculation results. It can be observed that the existence of initial air storage will have a significant impact on the hoisting cable tension. The hoisting cable tension becomes minimum when the head cover of the bucket

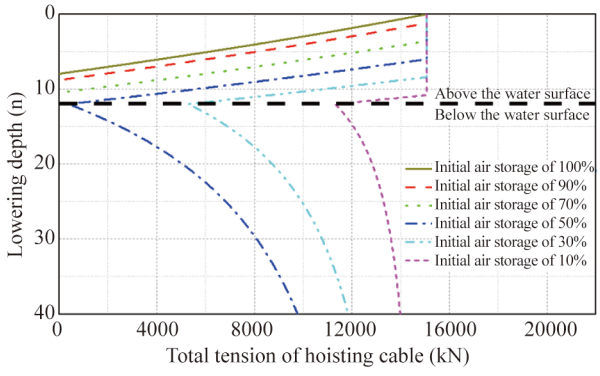

Fig. 2. Hoisting cable tension for different lowering depths.

is located on the water surface. When the initial air storage is above 50%, the buoyancy of the structure is too large, and the hoisting cable tension will be zero before the lowering depth reaches 12 m. At this time, the structure is in a self-floating state and the lowering fails. In addition, when the initial air storage is 50%, the total tension of the hoisting cable is only 380 kN. Therefore, the cable can relax easily under wave action.

As shown in Fig. 3, under the action of regular waves with a wave height of 2 m, period of 5 s and wave incident direction of 90°, the hoisting cable tension is equal to 0 in many cases according to Moses calculation. This signifies that the cable is relaxed, and the structure has a considerable impact on the cable after the relaxation. Therefore, when the initial air storage is 50%, the hoisting cable can relax easily under the action of waves although the hoisting cable is still under tension in still water. In this scenario, the lowering process is very likely to cause danger and become infeasible when the initial air storage is 50%. Thus, we study the initial air storage of 30% and 10% in this paper.

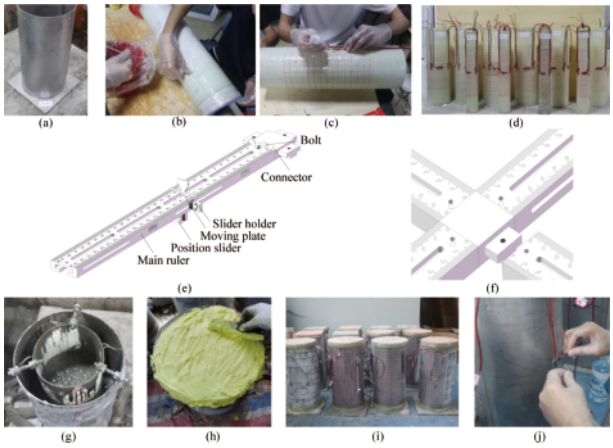

Fig. 3. Tension of each hoisting cable under wave action.

In summary, the percentage of initial air storage in the bucket volume β_0 should be carefully calculated, and it should not be excessively high in actual construction. The buoyancy should be smaller than the self-weight when the head cover of the bucket is on the water surface. Furthermore, the difference between the two should be guaranteed within a certain safety range.

All the bars and buckets in the jacket foundation are set as beam units in Moses. The bar unit is not flooded, which means that it can provide sufficient buoyancy. On the other hand, the suction bucket is flooded, which means that only the buoyancy generated by the bucket wall is considered, and the inner space of the bucket cannot provide buoyancy. The air cushion will be replaced by an equivalent simulation where a spring connected to the suction bucket is set.

In this paper, a three-bucket jacket foundation of an offshore wind farm is chosen as the research object. The overall height of the jacket foundation is 74 m, bottom foot distance is 30 m, and top foot distance is 17 m. The height and diameter of the bucket are both equal to 12 m. The overall mass of the foundation (M) is 1499 t, and the center of gravity is 26.68 m above the bottom of the bucket. The lifting lugs connected with the hoisting cable are located on the three main brackets. Two lugs extend out to the hoisting cables to merge into a single one, which simulates Cable A connected by the two hoisting cables (Cable C/D). The remaining lifting lug is attached to Cable B. Fig. 4 and Fig. 5 show the basic schematic diagram of the three-bucket jacket foundation and model diagram, respectively. In this paper, the hoisting cable arrangement shown in Fig. 5 is selected. Table 1 and Table 2 show the model parameters.

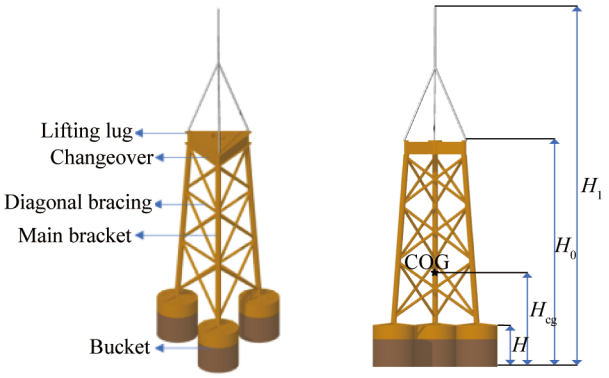

Fig. 4. Schematic diagram of the three-bucket jacket foundation.

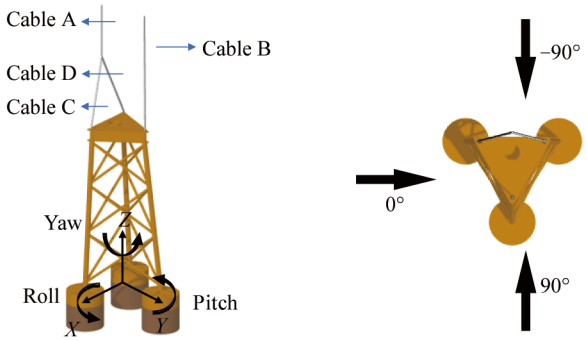

Fig. 5. Schematic diagram of the model and coordinate system.

Table 1 Structural parameters of three-bucket jacket foundation

H (m)	D (m)	H_0 (m)	H_{cg} (m)	M (t)	H_1 (m)
12	12	74	26.68	1499	100

Table 2 Hoisting cable parameters

Cable	Initial length (m)	Diameter (mm)	E-Modulus (MPa)	Damping (kNs/m)
Cable A	13.64			
Cable B	26	150	20000	140
Cable C/D	15			

In this paper, the elongation speed is added for Cable A and Cable B. The length of the hoisting cable increases with time and consequently, the structure can descend with time.

During the descending process, the wave condition is applied to the structure, and the complete time domain results of the movement and the cable tension can be obtained. The sensitivity analysis of the movement and cable tension is carried out in this paper according to the different variable values including spectral peak period, wave incident angle and initial air storage.

3 Time domain analysis of the lowering process in still water

First, the tension calculation results of the hoisting cable in still water with 30% and 10% initial air storage are compared, using the calculation results with 0% initial air storage as reference. Fig. 6 shows the calculation results. As the buoyancy of the bucket wall and bar is calculated, the tension of each cable decreases with time when the initial air storage is 0%. When the initial air storage values are 30% and 10%, the hoisting cable tension drops rapidly after the air in the bucket reaches the respective air storage capacity. The tensions slowly rise when the head cover of the bucket sinks below the water surface, which is consistent with the analysis carried out in Section 1. As shown in Fig. 7, by further comparing the calculated results of Eq. (5) with those of Moses, it can be gathered that the variation trends of the two are basically identical. However, results obtained using Eq. (5) are excessively high because they are calculated considering only the buoyancy of the air without taking the buoyancy of the bucket wall and bar into account. Furthermore, a large difference occurs when the head cover of the bucket is submerged in the water.

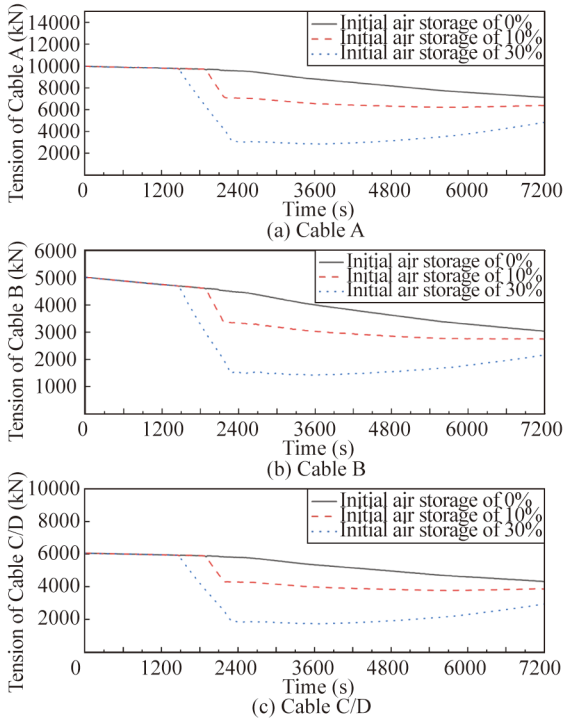

Fig. 6. Tension time history curve for different initial air storage values.

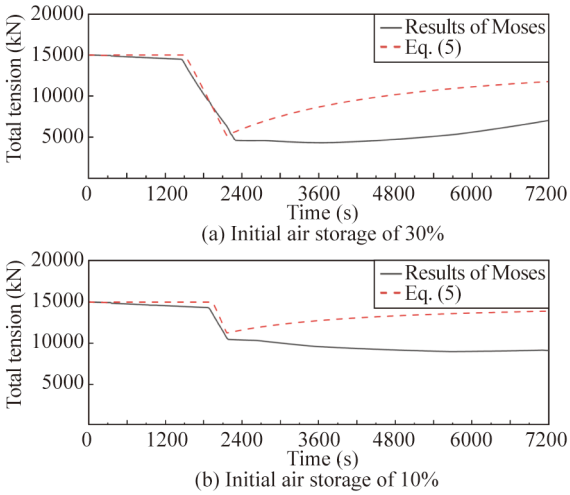

Fig. 7. Comparison of between results of Moses and Eq. (5).

When initial air storage is 10%, the total tension after the jacket foundation is lowered to the top cover submerged is obviously larger than that of the working condition with 30% initial air storage. This is due to the fact that 30% initial air storage provides more buoyancy to the foundation, thereby reducing sling tension.

4 Time domain analysis of the lowering process under the action of irregular waves

4.1 Wave incident direction

In this section, calculation results are shown with different initial air storage values and the wave incident direction is considered mainly for the time domain comparative analysis of the lowering process of three-bucket jacket foundation. The calculation results from the wave incident directions of −90° to 90° are only considered because the hoisting system composed of the structure and hoisting cable is arranged in a symmetrical fashion. Table 3 provides the specific calculation conditions.

Table 3 Calculation conditions

Condition	Lowering speed (m/h)	Spectral peak period (s)	H_s (m)	Wave incident direction (°)	Initial air storage (%)
1	20	5	2	−90	30
2					10
3				−60	30
4					10
5				−30	30
6					10
7				0	30
8					10
9				60	30
10					10
11				90	30
12					10

A significant wave height (H_s) of 2 m and spectral peak period of 5 s are considered. Time domain calculations are

performed by changing the wave incident direction. Figs. 8−11 show the calculation results of surge, sway, roll and pitch at the center of gravity of the three-bucket jacket

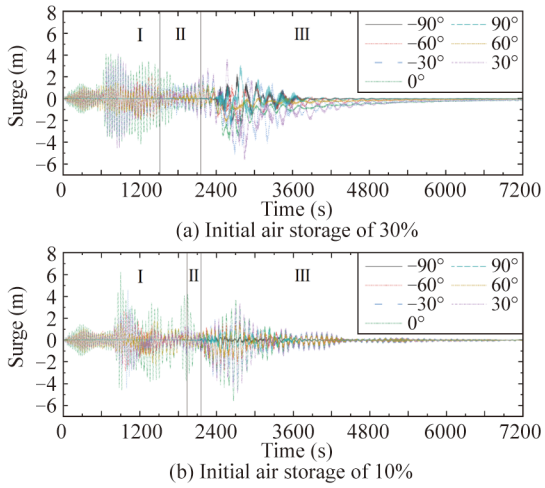

Fig. 8. Surge time series for different wave incident directions.

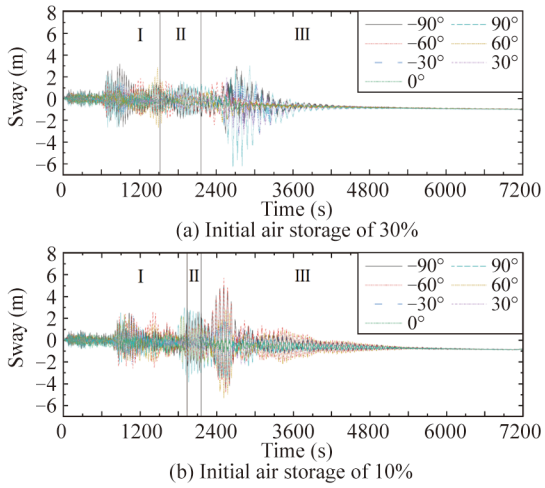

Fig. 9. Sway time series for different wave incident directions.

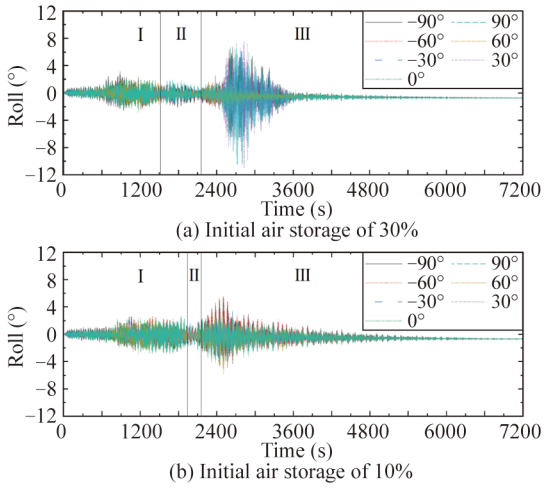

Fig. 10. Roll time series for different wave incident directions.

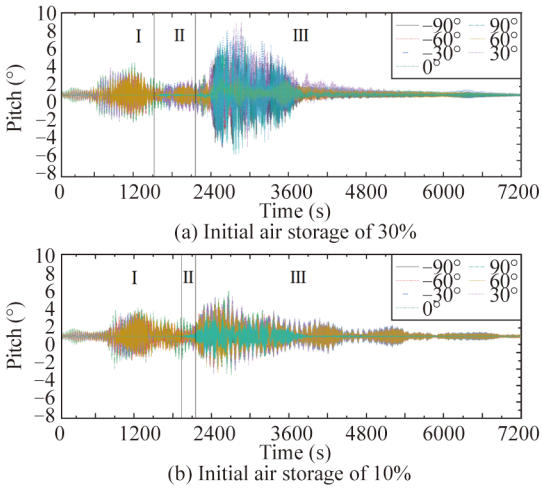

Fig. 11. Pitch time series for different wave incident directions.

foundation with different wave incident directions. In these figures, the initial air storage values of 30% and 10% are considered. In general, the motion response amplitude of the structure is larger in Stage I and the early phase of Stage III, but smaller in Stage II. In the middle and late phases of Stage III, the additional mass coefficient of the structure increases as the descending depth increases, and the motion amplitude of the structure gradually approaches zero. For surge and sway, the motion amplitude does not change significantly when the initial air storage values are 30% and 10%. On the other hand, for roll and pitch, the results with 30% initial air storage are higher than those with 10%. The motion response is stronger, especially at the beginning of Stage III. The sway and roll values do not recover at the end of lowering, but remain at a certain value smaller than zero. This may be because the stiffness and elongation of all the cables are not consistent at this lifting mode, which leads to the structural deviation.

When the wave incident direction are ±90°, the surge and pitch of the three-bucket jacket foundation remain basically zero before entering Stage III. However, after entering Stage III, obvious surge and pitch motions occur suddenly, which proves that the structure is relatively unstable in this stage. Similar behavior occurs for the sway and roll when the wave incident direction are ±30°.

Fig. 12 shows the statistical values of the motion responses of each degree of freedom for different wave incident directions. It can be observed that the maximum and minimum values of motion of the four degrees of freedom are correlated to the wave incident direction to a certain extent. The statistical results are basically consistent when the wave incident direction is symmetric about the horizontal axis. For the roll and pitch results, the absolute maximum and minimum values are smaller when the wave incident directions are ±60° and 0° under the condition of 30% initial air storage. The other values are larger, which proves that the roll and pitch motion responses are more sensitive to the

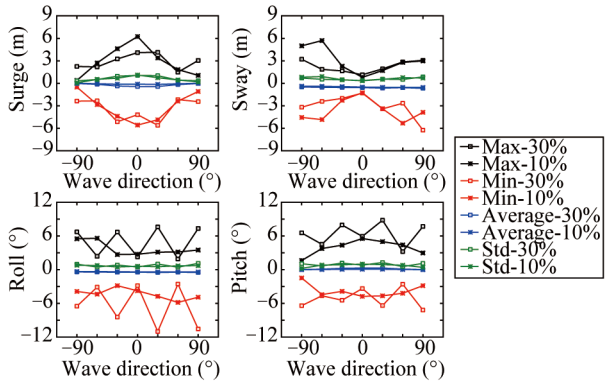

Fig. 12. Motion response statistics with different wave incident directions.

wave incident direction when the initial air storage is 30%.

Fig. 13 shows the vertical position of the bottom of the structure time series for different wave incident directions under two initial air storage conditions, considering the static water surface as the plane of origin. It can be observed that: (1) the heave response of the structure under the condition of 10% initial air storage is small, especially in the early part of Stage III; (2) the heave response of 30% is large, which may be because the buoyancy is large when the initial air storage is large, and the wave action on the structure is more likely to occur.

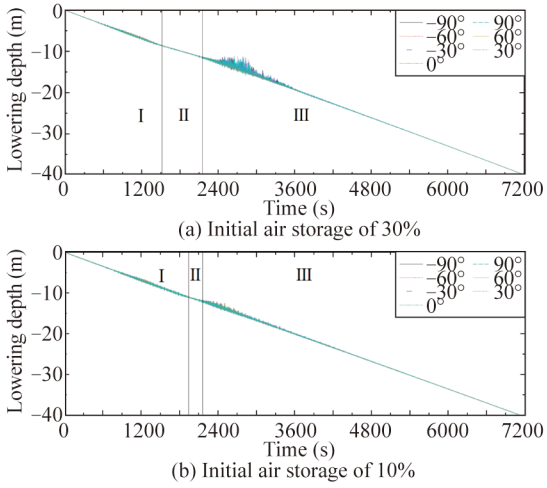

Fig. 13. Lowering depth time series for different wave incident directions.

The time domain calculation results of the tension of each hoisting cable are shown in Figs. 14−16 similar to the calculation results of the motion. The tension of the hoisting cable varies significantly in the early phases of Stages I and III, is smaller in stage II, and gradually stabilizes in the middle and late phases of Stage III. Therefore, during the hoisting construction process, the suction bucket structure is unstable in the water entry stage. This is because the structure is susceptible to the influence of wave force since a significant amount of movement occurs. As the lowering depth increases, the suction bucket with large diameter gradually

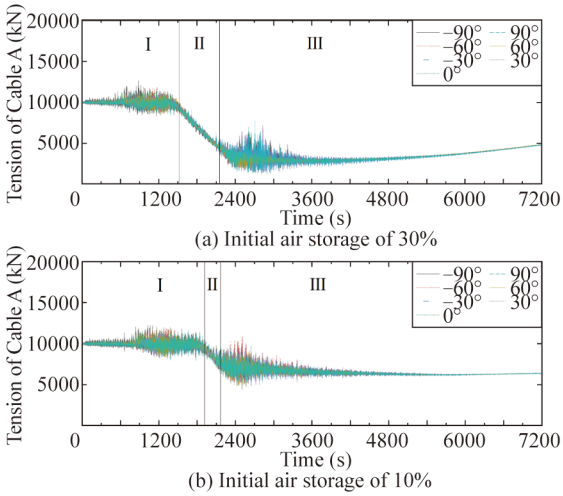

Fig. 14. Tension time series of Cable A for different wave incident directions.

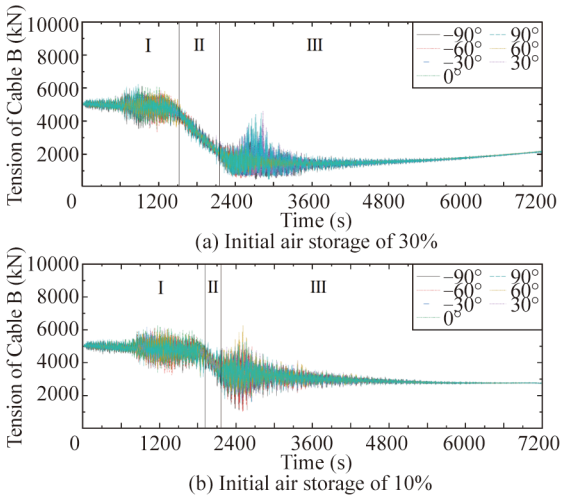

Fig. 15. Tension time series of Cable B for different wave incident directions.

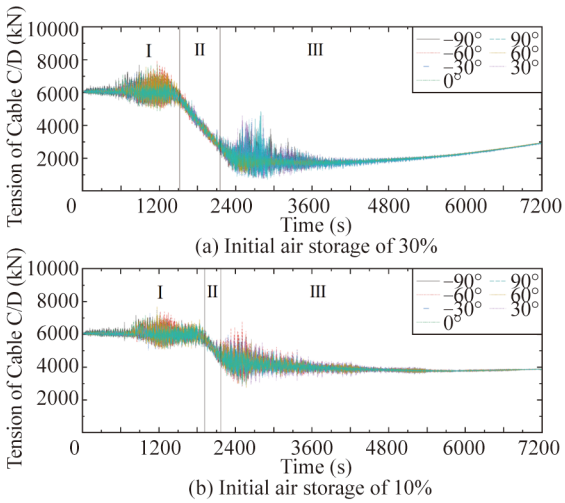

Fig. 16. Tension time series of Cable C/D for different wave incident directions.

moves away from the surface water area where the wave action occurs. The wave force can only act on the thinner jacket bar. Meanwhile, the additional mass coefficient also increases since the structure does not move easily and the variation range of the cable tension is also considerably reduced. Therefore, in the actual construction, special care should be taken to avoid danger when the suction bucket passes through the area of wave action.

The concept of dynamic amplification factor (f_d) is introduced in order to facilitate the comparison of the tension calculation results. f_d is equal to the ratio of the maximum hoisting cable tension to the weight of the structure. The Det Norske Veritas (DNV-RP-H103) (Det Norske Veritas, 2011) specification recommends that f_d should be smaller than 1.3 for offshore structures with a mass of 1000−2000 t. Similarly, as this paper studies, the use of air cushion structure to reduce the tension of the hoisting cable, the ratio of the minimum tension to the self-weight of the structure is also calculated in this section. To facilitate the comparison of the hoisting cable tension variation, the ratio between the maximum value of hoisting cable tension and the self-weight of the structure is defined as $f_{d\text{-}max}$, and the ratio between the minimum value of the hoisting cable tension and the self-weight of the structure is defined as $f_{d\text{-}min}$. Fig. 17 and Fig. 18 show the calculated results of these two ratios.

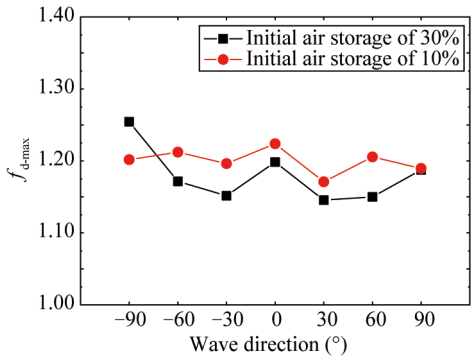

Fig. 17. $f_{d\text{-}max}$ for different wave incident directions.

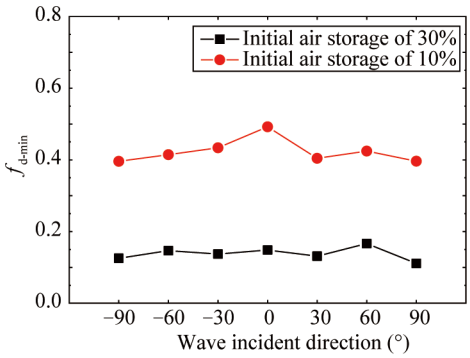

Fig. 18. $f_{d\text{-}min}$ for different wave incident directions.

Fig. 17 shows that $f_{d\text{-}max}$ fluctuates around 1.15 when the initial air storage is 10%. However, when the initial air storage is 30%, $f_{d\text{-}max}$ in other wave incident directions is smaller than the calculated result with 10% initial air storage except for the wave incident direction of 90°. These results prove that $f_{d\text{-}max}$ can be effectively reduced in the case of large air storage. However, it can be gathered from Fig. 18 that due to the high buoyancy in Stage III, the tension of the hoisting cable decreases considerably when the initial air storage is 30%. When the wave incident direction is 30°, the total tension of the hoisting cable is only 4% of the total structural weight. Therefore, although the hoisting cable tension can be effectively reduced when the initial air storage is 30%, the construction risk is relatively high.

4.2 Spectral peak period

The results shown in this section mainly consider the spectral peak period of waves for carrying out a time domain comparative analysis of the lowering process of the three-bucket jacket foundation with different initial air storage values. This section focuses on the spectral peak periods of 5, 7, 9 and 11 s, which are the common wave periods under actual sea conditions. At the same time, calculations are performed with initial air storage of 10% and 30%. Table 4 shows the specific calculation conditions.

Table 4 Calculation conditions

Condition	Lowering speed (m/h)	Spectral peak period (s)	H_s (m)	Wave incident direction (°)	Initial air storage (%)
1	20	5	2	90	30
2					10
3		7			30
4					10
5		9			30
6					10
7		11			30
8					10

The significant wave height is 2 m and the wave incident direction is 90°. Time domain calculations are carried out by changing the spectral peak period. Figs. 19−22 show the

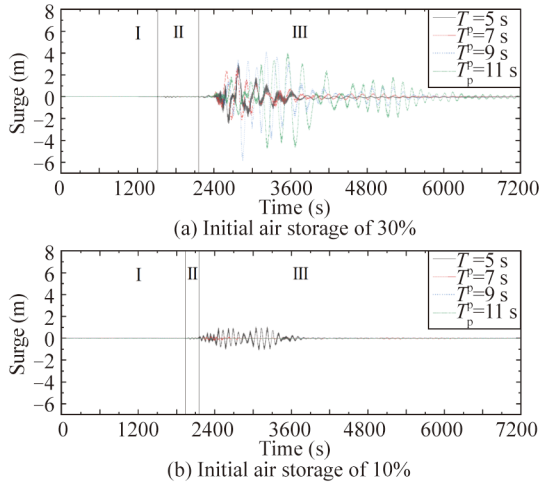

Fig. 19. Surge time series for different wave spectral peak periods.

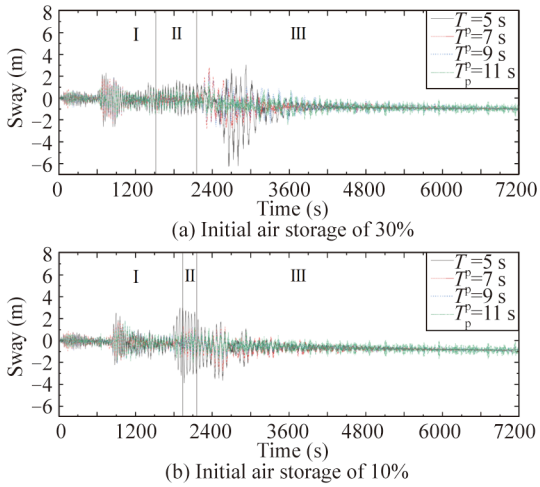

Fig. 20. Sway time series for different wave spectral peak periods.

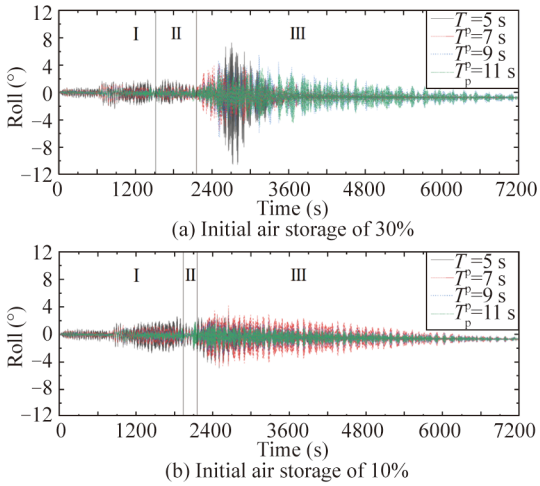

Fig. 21. Roll time series for different wave spectral peak periods.

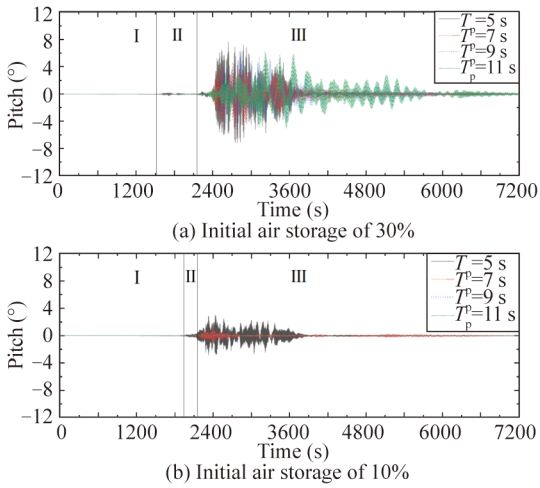

Fig. 22. Pitch time series for different wave spectral peak periods.

calculation results of the surgy, sway, roll and pitch motions of the center of gravity of the three-bucket jacket foundation. In these results, irregular wave action with different spectral peak periods and initial air storage values of 30% and 10% are considered. Generally speaking, the structure movement mainly occurs in the early phase of Stage III, whereas it is relatively small in Stage II. At the same time, in the middle and late phases of Stage III, the additional mass coefficient of the structure increases as the descending depth increases, and the motion amplitude of the structure gradually tends to zero. For the sway and pitch motions, the motion amplitude is basically zero in Stage I, slightly increases in Stage II, and increases sharply after the beginning of Stage III. The movement under each spectral peak period is more obvious when the initial air storage is 30%. Whereas, when the initial air storage is 10%, the movement amplitude is larger only when the spectral peak period is 5 s, unlike the behavior at he initial air storage of 30%. Similar to the previous section, sway and roll under the action of waves with different spectral peak periods do not return to zero at the end of the lowering process. Instead, they remain at a value smaller than zero, which again proves that such a situation should be independent with wave conditions.

Fig. 23 shows the motion response statistics under different wave spectral peak periods. It can be observed that the maximum and minimum values and standard deviations of motion responses in the four directions occur at the initial air storage of 30%, which proves that the motion response range at the initial air storage of 30% is large in all directions. Except for the extremum of the surge motion that increases with the increase of spectral peak period when the initial air storage is 30%, all other results decrease as the spectral peak period increases.

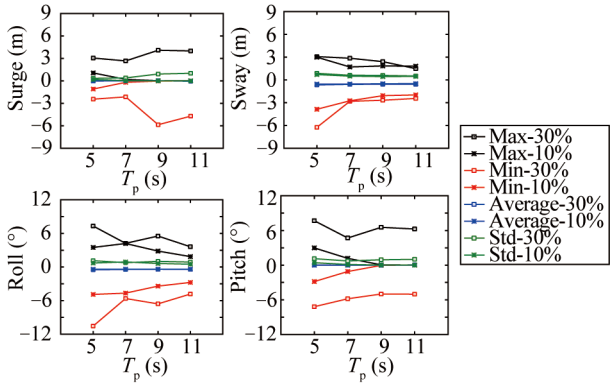

Fig. 23. Motion response statistics under different wave spectral peak periods.

Fig. 24 shows the curve of the vertical position of the center of gravity of the three-bucket jacket foundation with two different initial air storage and varying wave spectral peak periods. It can be observed that when the initial air storage is 30%, there is a large fluctuation in the early phase of Stage III. While, the heave amplitude is small in the other cases because the wave period is close to the natural period of the structure.

Figs. 25−27 show the time domain calculation results of

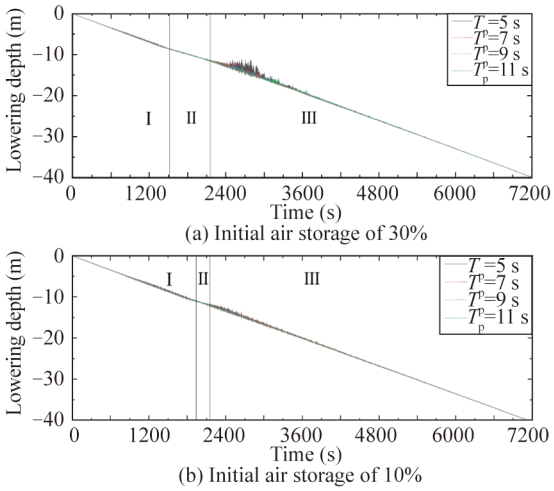

Fig. 24. Heave time series for different wave spectral peak periods.

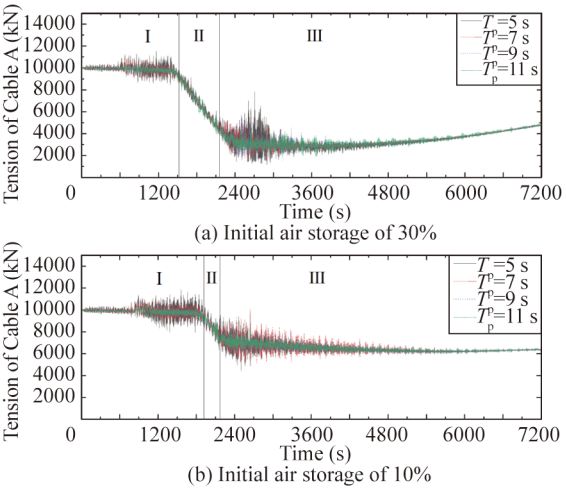

Fig. 25. Tension time series of Cable A for different wave spectral peak periods.

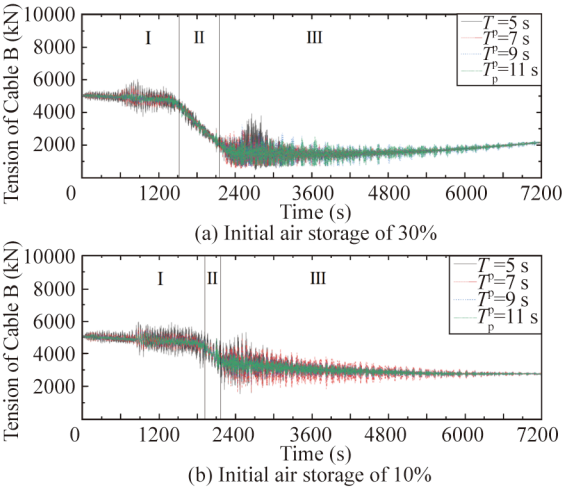

Fig. 26. Tension time series of Cable B for different wave spectral peak periods.

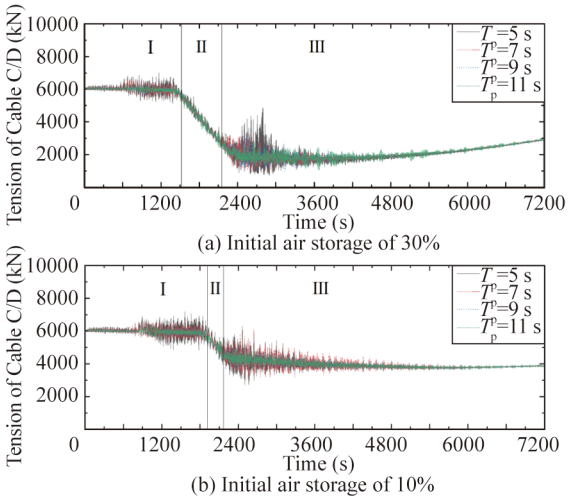

Fig. 27. Tension time series of Cable C/D for different wave spectral peak periods.

the tension of each hoisting cable. Similar to the calculation results of the motion response, the tension varies considerably in the early phases of Stages I and III, is smaller in Stage II, and gradually stabilizes in the middle and late phases of Stage III. In the actual construction, when the suction bucket passes through the wave action area and the wave period is concentrated at about 5 s, extra attention should be paid to avoid damage

Fig. 28 and Fig. 29 show the statistical ratios of the maximum and minimum values of the total tension of the

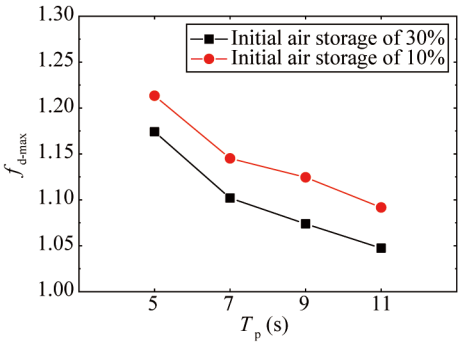

Fig. 28. $f_{d\text{-}max}$ for different wave spectral peak periods.

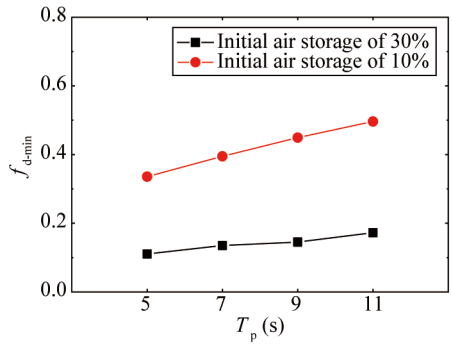

Fig. 29. $f_{d\text{-}min}$ for different wave spectral peak periods.

cable under different spectral peak periods, respectively. It can be observed from Fig. 28 that the dynamic coefficient with the initial air storage of 30% is smaller than that with the initial air storage of 10% in the same spectral peak period. The difference between the two is not significant when the spectral peak period is small; however, the difference slightly increases as the spectral peak period increases. In general, the dynamic coefficients with two air storage values decrease with the increase of spectral peak period. According to the above analysis, this behavior may be related to the difference between the wave period and the natural period of the whole hoisting system to some extent. It can be observed from Fig. 29 that $f_{\text{d-min}}$ has little correlation with the spectral peak period. When the initial air storage is 30%, the minimum tension of the cable is significantly lower than that with the initial air storage of 10%. Therefore, in combination with the analysis in Section 3.1, it can be concluded that for the initial air storage of 30% and under the action of the irregular wave with a significant wave height of 2 m, the cable relaxation does not occur but is already very close to zero. Once a big wave is encountered, it is likely to be dangerous and, therefore, this method of launching is still not recommended in actual projects.

5 Conclusions

This article was based on the Moses calculation model of the three-bucket jacket foundation of offshore wind turbine. The time domain simulation of the whole three-bucket jacket foundation lowering process was carried out. The effects of different environmental conditions and initial gas storage on the structural movement and the tension of the hoisting cable were studied. The main conclusions of this paper are as follows.

(1) The time domain calculations of the hoisting cable tension with the lowering speed of 20 m/h and the initial air storage values of 0%, 10% and 30% were carried out. The variation trend of the calculation results was basically the same as the analysis of theory, but the calculation results obtained by theory are excessively high because the buoyancy of the bucket wall and bar was considered.

(2) By comparing the calculation results for different wave incident directions, it was concluded that when the wave incident direction was symmetrical about the *X*-axis, the statistical results were basically the same. The responses of the roll and pitch were more sensitive to the wave incident direction when the initial air storage was 30%.

(3) The larger initial air storage in the bucket can effectively reduce f_{d} and the maximum tension. When the initial air storage was 10%, $f_{\text{d-max}}$ fluctuated around 1.15, while when the initial air storage was 30%, $f_{\text{d-max}}$ in wave incident directions other than 90° was smaller than the calculated result with the initial air storage of 10%. However, when the initial air storage was 30%, the tension of the hoisting cable decreased significantly. In this case, the tension is very easy to relax, resulting in a larger impact force, and the construction risk was large.

(4) By comparing the calculation results for different spectral peak periods, it was observed that the motion response amplitude was larger when the initial air storage was 30%. All the other results decreased with the increase of spectral peak period, except for the maximum value of surge motion. $f_{\text{d-max}}$ decreased with the increase of the spectral peak period, while the minimum value of the hoisting cable tension had little correlation with the spectral peak period.

References

Bertelsen, T.Ø., 2014. *Installation of Large Subsea Structures*: *Lowering of Suction Anchors Through the Splash Zone*, NTNU, Trondheim.

Cheung, K.F., Phadke, A.C., Smith, D.A., Lee, S.K. and Seidl, L.H., 2000. Hydrodynamic response of a pneumatic floating platform, *Ocean Engineering*, 27(12), 1407–1440.

Det Norske Veritas, 2011. *Modelling and Analysis of Marine Operations*, Det Norske Veritas.

Gordon, R.B., Grytøyr, G. and Dhaigude, M., 2013. Modeling suction pile lowering through the splash zone, *Proceedings of ASME 2013 32nd International Conference on Ocean*, *Offshore and Arctic Engineering*, ASME, Nantes, France.

He, F., Huang, Z.H. and Wing-Keung Law, A., 2012. Hydrodynamic performance of a rectangular floating breakwater with and without pneumatic chambers: An experimental study, *Ocean Engineering*, 51, 16–27.

He, F., Huang, Z.H. and Wing-Keung Law, A., 2013. An experimental study of a floating breakwater with asymmetric pneumatic chambers for wave energy extraction, *Applied Energy*, 106, 222–231.

Henriques, J.C.C., Falcão, A.F.O., Gomes, R.P.F. and Gato, L.M.C., 2013. Latching control of an oscillating water column spar-buoy wave energy converter in regular waves, *Journal of Offshore Mechanics and Arctic Engineering*, 135(2), 021902.

Ikoma, T., Masuda, K., Maeda, H. and Rheem, C.K., 2002. Hydroelastic behavior of air-supported flexible floating structures, *Proceedings of ASME 2002 21st International Conference on Offshore Mechanics and Arctic Engineering*, ASME, Oslo, Norway.

Ikoma, T., Masuda, K., Omori, H., Osawa, H. and Maeda, H., 2013. Improvement of wave power take-off performance due to the projecting walls for OWC type WEC, *Proceedings of ASME 2013 32nd*

International Conference on Ocean, *Offshore and Arctic Engineering*, ASME, Nantes, France.

Ikoma, T., Masuda, K., Rheem, C.K. and Maeda, H., 2012. Hydroelastic behaviors of VLFS supported by many aircushions with the three-dimensional linear theory, *Journal of Offshore Mechanics and Arctic Engineering*, 134(1), 011104.

Koo, W., 2009. Nonlinear time–domain analysis of motion-restrained pneumatic floating breakwater, *Ocean Engineering*, 36(9–10), 723–731.

Pinkster, J.A., 1997. The effect of air cushions under floating offshore structures, *Proceedings of the Eighth International Conference on the Behaviour of Offshore Structures*, Delft Univ. of Technology, Delft, The Netherlands, pp. 143–158.

Pinkster, J.A., Fauzi, A., Inoue, K. and Tabeta, S., 1998. *The Behaviour of Large Air Cushion Supported Structures in Waves*, Yomei, Fukuoka, pp. 497–509.

Seidl, L.H., 1980. *Development of An ASP* (*Air Stabilized Platform*), National Technical Information Service.

Shi, W., Zhang, L.X., Karimirad, M., Michailides, C., Jiang, Z.Y. and Li, X., 2023. Combined effects of aerodynamic and second-order hydrodynamic loads for floating wind turbines at different water depths, *Applied Ocean Research*, 130, 103416.

Tassin, A., Piro, D.J., Korobkin, A.A., Maki, K.J. and Cooker, M.J., 2013. Two-dimensional water entry and exit of a body whose shape varies in time, *Journal of Fluids and Structures*, 40, 317–336.

Thiagarajan, K.P. and Morris-Thomas, M.T., 2006. Wave-induced motions of an air cushion structure in shallow water, *Ocean Engineering*, 33(8–9), 1143–1160.

van Kessel, J.L.F., 2010. Aircushion supported mega-floaters, *SWZ Maritime*, 4(131), 22–25.

Zhang, Y., Shi, W., Li, D.S., Li, X., Duan, Y.F. and Verma, A.S., 2022. A novel framework for modeling floating offshore wind turbines based on the vector form intrinsic finite element (VFIFE) method, *Ocean Engineering*, 262, 112221.

Zou, M.Y., Chen, M.S., Zhu, L., Li, L. and Zhao, W.H., 2023. A constant parameter time domain model for dynamic modelling of multi-body system with strong hydrodynamic interactions, *Ocean Engineering*, 268, 113376.